Crystalline Ionic Solutions*

Francis K. Fong, Robert L. Ford, and Richard H. Heist
Department of Chemistry, Purdue University, Lafayette, Indiana 47907
(Received 6 March 1970)

Systems of crystalline ionic solutions containing impurity cations and associated compensation defects are described. Interactions between aliovalent ions and compensation defects give rise to configuration partition functions which predict a distribution in ion-defect pair separation distances at low temperatures. At elevated temperatures such ion-defect pairs dissociate, and the concept of pair formation more appropriately gives way to the concept of pair correlation functions. The relative sizes of the aliovalent ion and the host ion which it replaces are seen to exert a pronounced effect on pair distribution. Salient features of the theory are applied to the KCl : Sr^{2+}, NaCl : Mn^{2+}, NaCl : Sr^{2+}, LiCl : Mn^{2+} and (alkaline-earth halide): (rare earth)$^{3+}$ systems. While the high-temperature treatment lends itself to comparisons with the Debye-Hückel theory for electrolytes, the low-temperature pair distribution theory is shown to be valid chiefly because of the specific nature of the crystalline ionic solutions.

I. INTRODUCTION

The law of equilibrium distribution which governs the low-temperature pair formation of divalent cations and cation vacancies in alkali halides[1] and that of trivalent cations and interstitial anions in alkaline-earth halides[2] has been useful in the interpretation and prediction of spectroscopic data on compensated lattices,[2,3-6] in which aliovalent cations and lattice defects interact as ions of opposite unit charges in a crystalline solution. In general, N_i unipositive ions and N_i uninegative ions give rise to a total interaction energy, for a given configuration,

$$U(\hat{R}_1, \hat{R}_2, \ldots, \hat{R}_{2N_i}) = \sum_{1 \le i < j \le N_i} \cdots \sum {}^{+}u(\hat{R}_{ij}) + \sum_{N_i+1 \le l < m \le 2N_i} \cdots \sum {}^{+}u(\hat{R}_{lm}) + \sum_{\substack{1 \le k \le N_i \\ N_i+1 \le p \le 2N_i}} \cdots \sum {}^{-}u(\hat{R}_{kp}), \quad (1)$$

where $\hat{R}_1, \hat{R}_2, \ldots, \hat{R}_{2N_i}$ are the position vectors of the N_i cations and N_i anions and ${}^{+}u$ and ${}^{-}u$ denote repulsive and attractive interaction energies, respectively. At low temperatures at which only the attractive terms are important, it has been shown that the canonical configuration partition function

$$Z = \sum_{\text{a.c.}} \exp[-U(\hat{R}_1, \hat{R}_2, \ldots, \hat{R}_{2N_i})/kT], \quad (2)$$

where a.c. denotes all configurations, reduces to a product of "molecular" pair parition functions, such that[1]

$$Z \cong \Omega_p \left(\sum_{l=1}^{l=l'} g_l e^{-{}^{-}u(R_l)/kT} \right)^{N_i} = \Omega_p q_p^{N_i}, \quad (3)$$

where g_l is the number of equivalent positions at which a defect (i.e., a uninegative ion) can be situated about an aliovalent cation (i.e., a unipositive ion) at a separation distance of R_l. The index l denotes the number of nearest-neighbor separation, and $R_l = (2l)^{1/2}\, a$ in alkali halides[1] and $R_l = (2l-1)^{1/2}\, a$ in alkaline-earth halides,[2] a being a characteristic lattice parameter for the host crystal.[1,2] The sum over l is carried from $l = 1$ to $l = l'$, where l' is arbitrarily chosen such that q_p does not change appreciably in summing beyond l'. Ω_p is the number of ways of placing N_i ion-defect pairs in a finite host lattice. At a given temperature for which Eq. (3) is valid, the number n_l^* of pairs of separation R_l is

$$n_l^* = N_i q_p^{-1} g_l e^{-{}^{-}u(R_l)/kT}, \quad (4)$$

which has been shown to be the case in the KCl: Sm^{2+}[1,3] and the CaF_2:RE^{3+} (RE denotes rare earth[2]) systems at appropriately low temperatures. At high temperatures at which the ion-defect pairs dissociate to an appreciable extent, Eqs. (3) and (4) become meaningless as we must include the repulsive terms in Eq. (1) in our evaluation of Z.

The purpose of the present work is threefold: (a) to generalize the treatment of ionic solutions in crystalline lattices by extending the consideration of Z to high temperatures; (b) to extend the distribution calculation to several crystalline ionic solution systems and thereby examine the effect of the relative sizes of the aliovalent ion and the host ion upon the distribution of pair formation; and (c) to clarify the validity of Eq. (3), which results from a conceptual argument rather than a rigorous derivation. Differences as well as similarities between our treatment of the crystalline ionic solutions and that (e.g., the Debye-Hückel theory) of ionic solutions in fluid states will be emphasized.

II. HIGH-TEMPERATURE PARTITION FUNCTION AND PAIR CORRELATION FUNCTION

In rewriting Eq. (2) for the configuration partition function at high temperature, and in taking into account all the attractive and repulsive terms, we define the following quantities as a measure of departure from ideality (i.e., the absence of interactions between the ions):

$$^{+}f_{ij} = e^{-{}^{+}u(\hat{R}_{ij})/kT} - 1,$$
$$^{+}f_{lm} = e^{-{}^{+}u(\hat{R}_{lm})/kT} - 1, \tag{5}$$

and

$$^{-}f_{kp} = e^{-{}^{-}u(\hat{R}_{kp})/kT} - 1,$$

such that

$$Z = \sum_{\text{a.c.}} \prod (1 + {}^{+}f_{ij})(1 + {}^{+}f_{lm})(1 + {}^{-}f_{kp}) \quad . \tag{6}$$

For a given configuration,

$$e^{-U(\hat{R}_1, \hat{R}_2, \cdots, \hat{R}_{2N_i})/kT} = \prod (1 + {}^{+}f_{ij})(1 + {}^{+}f_{lm})(1 + {}^{-}f_{kp})$$
$$= 1 + \sum {}^{+}f_{ij} + \sum {}^{+}f_{lm} + \sum {}^{-}f_{kp} + \sum {}^{+}f_{ij}\,{}^{+}f_{i'j'} + \sum {}^{+}f_{lm}\,{}^{+}f_{l'm'}$$
$$+ \sum {}^{-}f_{kp}\,{}^{-}f_{k'p'} + \sum {}^{+}f_{ij}\,{}^{-}f_{kp} + \sum {}^{+}f_{lm}\,{}^{-}f_{kp} + \sum {}^{+}f_{ij}\,{}^{+}f_{lm}$$
$$+ \text{higher terms} , \tag{7}$$

where there are $\frac{1}{2}N_i(N_i - 1)$ identical terms in $\sum {}^{+}f_{ij}$ which is identical to $\sum {}^{+}f_{lm}$, N_i^2 in $\sum {}^{-}f_{kp}$, $\frac{1}{8}N_i^4$ in $\sum {}^{+}f_{ij}\,{}^{+}f_{i'j'}$ which is identical to $\sum {}^{+}f_{lm}\,{}^{+}f_{l'm'}$, $\frac{1}{2}N_i^4$ in $\sum {}^{-}f_{kp}\,{}^{-}f_{k'p'}$, $\frac{1}{2}N_i^4$ in $\sum {}^{+}f_{ij}\,{}^{-}f_{kp}$ which is identical to $\sum {}^{+}f_{lm}\,{}^{-}f_{kp}$, and $\frac{1}{4}N_i^4$ in $\sum {}^{+}f_{ij}\,{}^{+}f_{lm}$. The meaning of the sum of $^{+}f_{ij}$ over all configurations

$$\sum_{\text{a.c.}} {}^{+}f_{ij} = \sum_{\text{a.c.}} (e^{-{}^{+}u(\hat{R}ij)/kT} - 1) \tag{8}$$

can be examined in the following manner: For a given fixed $\hat{R}_{ij}$, there are Ω' ways of arriving at all possible ways of arranging the remaining $2(N_i - 1)$ ions, such that

$$\sum_{\text{a.c.}} {}^{+}f_{ij} = \Omega' \sum_{\hat{R}_{ij}} (e^{-{}^{+}u(\hat{R}_{ij})/kT} - 1), \tag{9}$$

where the sum is carried over all possible values for $\hat{R}_{ij}$. Fixing the position of the ith ion as the center of our new coordinate system, we have $R_{ij} = R_j$, the distance of separation of the jth ion measured from the origin,

$$\sum_{\text{a.c.}} {}^{+}f_{ij} = \Omega \sum_{R_j} g_j (e^{-{}^{+}u(R_j)/kT} - 1) \quad , \tag{10}$$

where g_j is the number of equivalent positions about the ith ion (i.e., the origin) at R_j. The prime on Ω has been dropped due to the coordinate transformation. The determination of Ω can be made by realizing the fact that

$$\Omega \sum_j g_j = \Omega_0 (2N_i, N) \quad , \tag{11}$$

where $\Omega_0(2N_i, N)$ is, for example, the total number of configurations for the random mixing of $2N_i$ ions on N available lattice sites as in KCl:Sm^{2+}

$$\Omega_0 (2N_i, N) = N!/(N_i!)^2 (N - 2N_i)! \quad . \tag{12}$$

Since $\sum_j g_j = N - 1$, we obtain

$$\Omega = N!/(N_i!)^2 (N - 2N_i)!\,(N - 1) \quad . \tag{13}$$

Further analysis of the terms in Eq. (6) in terms of Ω, g_j, N_i, N, ^{+}u, and ^{-}u, readily leads to the following expression for the configuration partition function in the case $N_i/N \ll 1$:

$$Z = \Omega_0 (2N_i, N) \left(1 + \frac{N_i}{(N-1)} \left[\sum_j g_j (e^{-{}^{+}u(R_j)/kT} - 1) \right.\right.$$
$$\left.\left. + \sum_p g_p (e^{-{}^{-}u(R_p)/kT} - 1) \right] \right)^{N_i} + \text{"other terms"} , \tag{14}$$

where the contribution of the "other terms" becomes negligibly small[7] for a dilute system in which which $N_i/N \ll 1$. Neglecting the "other terms" in Eq. (14), we write for the internal energy due to configuration interaction,

$$\overline{U} = kT^2 \frac{\partial \ln Z}{\partial T} = \frac{N_i^2}{zN} \sum_l g_l (e^{-u_l/kT} - e^{u_l/kT}) \left(u_l - T \frac{\partial u_l}{\partial T} \right) , \tag{15}$$

where

$$z = 1 + \frac{N_i}{N} \left\{ 2 \sum_l g_l \left[\cosh\left(\frac{u_l}{kT} \right) - 1 \right] \right\} = 1 + \frac{N_i}{N} S \tag{16}$$

and

$$u_l = {}^{+}u(R_l) = -{}^{-}u(R_l).$$

From Eq. (2), we obtain

$$\overline{U} = \frac{kT^2}{Z} \frac{\partial}{\partial T} \sum_{\text{a.c.}} e^{-U(\hat{R}_1, \hat{R}_2 \cdots, \hat{R}_{2N_i})/kT}$$
$$= \frac{1}{Z} \sum \left(U - T \frac{\partial U}{\partial T} \right) e^{-U/kT} \quad . \tag{17}$$

Upon substitution of Eq. (1) in Eq. (17),

$$\overline{U} = \frac{1}{Z} \sum_{\text{a.c.}} \left[\left[2 \sum_i \sum_j {}^{+}u(\hat{R}_{ij})\, e^{-U/kT} + \sum_k \sum_p {}^{-}u(\hat{R}_{kp}) e^{-U/kT} \right] \right.$$
$$\left. - T \left(2 \sum_i \sum_j \frac{\partial\, {}^{+}u(\hat{R}_{ij})}{\partial T} e^{-U/kT} + \sum_k \sum_p \frac{\partial\, {}^{-}u(\hat{R}_{kp})}{\partial T} e^{-U/kT} \right) \right] . \tag{18}$$

Since there are $N_i(N_i - 1) \sim N_i^2$ identical terms in $\sum_i \sum_j {}^{+}u(\hat{R}_{ij})\, e^{-U/kT}$ and N_i^2 identical terms in $\sum_k \sum_p {}^{-}u(\hat{R}_{kp})\, e^{-U/kT}$, we rewrite Eq. (18) in the equivalent form (replacing $\hat{R}_{ij}$ by $\hat{R}_{12}$ and $\hat{R}_{kp}$ by $\hat{R}_{1(N_i+1)}$),

$$\bar{U}=\frac{N_i^2}{Z}\Bigg[\sum_{\hat{R}_1}\sum_{\hat{R}_2}{}^{+}u(\hat{R}_{12})\sum_{\hat{R}_3,\hat{R}_4\cdots\hat{R}_{2N_i}}\cdots\sum e^{-U(\hat{R}_1,\hat{R}_2,\ldots,\hat{R}_{2N_i})/kT}$$

$$+\sum_{\hat{R}_1}\sum_{\hat{R}_{(N_i+1)}}{}^{-}u(\hat{R}_{1(N_i+1)})$$

$$\times\sum_{\substack{\hat{R}_2,\hat{R}_3,\cdots,\hat{R}_{N_i}\\ \hat{R}_{(N_i+2)},\cdots,\hat{R}_{2N_i}}}\cdots\sum e^{-U(\hat{R}_1,\hat{R}_2,\cdots,\hat{R}_{2N_i})/kT}$$

$$-T\Bigg(\sum_{\hat{R}_1}\sum_{\hat{R}_2}\frac{\partial\,{}^{+}u(\hat{R}_{12})}{\partial T}\sum_{\hat{R}_3,\hat{R}_4,\cdots,\hat{R}_{2N_i}}\cdots\sum e^{-U(\hat{R}_1,\hat{R}_2,\cdots,\hat{R}_{2N_i})/kT}$$

$$+\sum_{\hat{R}_1}\sum_{\hat{R}_{(N_i+1)}}\frac{\partial\,{}^{-}u(\hat{R}_{1(N_i+1)})}{\partial T}$$

$$\times\sum_{\substack{\hat{R}_2,\hat{R}_3,\cdots,\hat{R}_{N_i}\\ \hat{R}_{(N_i+2)},\cdots,\hat{R}_{2N_i}}}\cdots\sum e^{-U(\hat{R}_1,\hat{R}_2,\cdots,\hat{R}_{2N_i})/kT}\Bigg)\Bigg] \quad . \tag{19}$$

We now define the generic distribution functions $\rho^{(2)}$:

$${}^{+}\rho^{(2)}(\hat{R}_{12})=N_i^2\,{}^{+}P^{(2)}(\hat{R}_{12})$$

$$=\frac{N_i^2}{Z}\sum_{\hat{R}_3,\hat{R}_4,\cdots\hat{R}_{2N_i}}\cdots\sum e^{-U(\hat{R}_1,\hat{R}_2,\cdots,\hat{R}_{2N_i})/kT} \quad , \tag{20a}$$

$${}^{-}\rho^{(2)}(\hat{R}_{1(N_i+1)})=N_i^2\,{}^{-}P^{(2)}(\hat{R}_{1(N_i+1)})$$

$$=\frac{N_i^2}{Z}\sum_{\substack{\hat{R}_2,\hat{R}_3,\cdots\hat{R}_{N_i}\\ \hat{R}_{(N_i+2)},\cdots\hat{R}_{2N_i}}}\cdots\sum e^{-U(\hat{R}_1,\hat{R}_2,\cdots,\hat{R}_{2N_i})/kT} \quad , \tag{20b}$$

where ${}^{+}P^{(2)}(\hat{R}_{12})$ is the specific distribution function giving the probability of finding the second like ion at $\hat{R}_2$ with the first at $\hat{R}_1$, the sum being carried over all possible position vectors for the remaining $(2N_i-2)$ ions, and ${}^{-}P^{(2)}(\hat{R}_{1(N_i+1)})$ has the same meaning for two ions of opposite charges. The pair correlation function, or the radial distribution function is given as

$$G(R_{12})=(N/N_i)^2\rho^{(2)}(R_{12}) \quad . \tag{21}$$

Performing a coordinate transformation fixing a cation as the center of origin,

$${}^{\pm}G(R_l)=(N/N_i)^2\,{}^{\pm}\rho^{(2)}(R_l) \quad , \tag{22}$$

where the + and − signs denote the charge of the second ion that is R_l away from the origin. Upon substitution of Eq. (22) in Eq. (19), we obtain

$$\bar{U}=\frac{N_i^2}{N}\sum_l u_l - T\frac{\partial u_l}{\partial T}\left[{}^{+}G(R_l)-{}^{-}G(R_l)\right] \tag{23}$$

having made use of the identity

$$\sum_{\hat{R}_1,\hat{R}_2}\equiv N\sum_l \quad .$$

Comparison of Eqs. (15) and (23) yields

$${}^{\pm}G(R_l)=z^{-1}g_l e^{\mp u_l/kT} \quad , \tag{24}$$

which gives a measure of the probability of finding a + or − ion at a distance R_l from the center of origin.

There is the probability $[N_i/(N-1)]\,{}^{\pm}G(R_l)$ of placing one of the N_i + or − ions at a distance R_l from the central positive ion. Since there are N_i positive ions, the total number ${}^{\pm}n_l^*$ of pair interactions at R_l is given by

$${}^{\pm}n_l^*=\frac{N_i^2}{N-1}\,{}^{\pm}G(R_l)=\frac{N_i^2}{(N-1)z}g_l e^{\mp u_l/kT} \quad . \tag{25}$$

The total number of attractive interactions at all values of R_l is N_i^2, i. e. , from Eq. (25),

$$\sum_l {}^{-}n_l^*=N_i^2=\frac{N_i^2}{(N-1)z}\sum_l g_l e^{-u_l/kT}, \tag{26}$$

such that

$$\sum_l g_l e^{-u_l/kT}=(N-1)z=q \quad . \tag{27}$$

This is true only when $u_l<kT$ for most important values of R_l, when $q\sim(N-1)$ and $z\sim 1$. The resulting condition from the definition of z in Eq. (16) is

$$S=2\sum_l g_l\left[\cosh\left(\frac{u_l}{kT}\right)-1\right]\ll\frac{N}{N_i} \quad . \tag{28}$$

In Sec. III, we shall make sample calculations of ${}^{\pm}n_l^*$ according to Eq. (25).

III. INTERACTION POTENTIAL AND CONVERGENCE

In the evaluation of Z in Eq. (14), we have ${}^{\pm}u_l=\pm e^2/\epsilon R_l$ (except for the nearest-neighbor interactions which are briefly described in Sec. IV), where e is the electrostatic unit and ϵ is the macroscopic dielectric constant of the crystalline lattice. In neglecting the "other terms" in Eq. (14) in arriving at Eq. (25), however, we have in essence overlooked the presence of all the other ions in our consideration of the interactions between given pairs of ions. As a result of this, it can be easily shown that S in Eq. (28) diverges unless a screen e^{-bR_l} is invoked for Coulombic interactions at large R_l as in the Debye-Hückel theory, where $b=(8\pi N_i e^2/\epsilon VkT)^{1/2}$, V being the volume of the system.

In the numerical evaluation of Z, we need to define u_l for all values of R_l. We assume that when $u_l/kT\leq 0.1$, $u_l=(e^2/\epsilon R_l)e^{-bR_l}$. At $l=1$ and 2, polarization effects as well as Coulombic in-

teractions must be taken into consideration in the evaluation of u_1 and u_2.[1,8] At $l=3$, we assume purely Coulombic interaction which is reasonable in view of the previous investigations.[1,2] In the intermediate region $R_3 \leq R_l \leq R_m$, where R_m is the value of R_l at which $u_m/kT \sim 0.1$, u_l is assumed to have the following form

$$u_l = \frac{e^2}{\epsilon R_l} \exp[-bR_l e^{-(R_m - R_l)(R_l - R_3)^{-1}}], \qquad (29)$$

which provides a smooth interpolation from the screened Coulombic interaction at $R_l \geq R_m$ to the pure Coulombic interaction at R_3. By employing the appropriate lattice descriptions for g_l as a function of l,[1,2] the configuration partition function Z in Eq. (14) has been evaluated in sum up to $l=1350$ ($R_{1350}=163.16$ Å) with a CDC 6500 computer for the CaF_2:RE^{3+} ($\epsilon=6.7$, $u_1=-0.477$ eV, and $u_2=-0.300$ eV)[2] and the KCl:Sr^{2+} ($\epsilon=5.03$, $u_1=-0.39$ eV, and $u_2=-0.50$ eV)[9] systems. The dependence of

$$z=[\Omega_0^{-1}(2N_i, N)Z]^{1/N_i} \qquad (30)$$

on N_i and T is given in Fig. 1 in the region for $1 \leq z \leq 1.2$. Some typical calculations are listed in Table I. From Eq. (25), ${}^{\pm}n_l^*$ has been calculated for CaF_2:RE^{3+} at $T=900$, 1100, 1300, 1500, and 1700 K with $N_i=10^{17}$ cm^{-3}. The results of this calculation are shown in Figs. 2 and 3 for $l \leq 21$. In sharp contrast with the low-temperature distribution curves,[2] in which practically *all* the cations are paired with associated compensation defect anions, we observe from Fig. 2 that in the high-temperature case under conditions specified above, only a small fraction (10^{-3}–10^{-2}) of the cations are in close association with the compensation defects. ${}^{+}n_l^*$ is several orders of magnitude lower than ${}^{-}n_l^*$ at small l, which is to be expected. Clearly, ${}^{+}n_l^*/{}^{-}n_l^*$ increases exponentially with T, approaching unity as $Z \to \Omega_0(2N_i, N)$. Moreover, at $R_l \gg R_m$,

$${}^{-}n_l^* \cong {}^{+}n_l^* \cong [N_i^2/(N-1)z]g_l, \qquad (31)$$

which follows from Eq. (25) since $u_l/kT \sim 0$ at $R_l \gg R_m$. For $N_i=10^{17}$ cm^{-3}, ${}^{-}n_l^* \sim {}^{+}n_l^* \sim 10^{12} g_l$.

TABLE I. Some sample calculations of R_m, $S=2\sum_l g_l[\cosh(\mu_l/kT)-1]$, and $z=1+(N_i/N)S$ for KCl:Sr^{2+} and CaF_2:RE^{3+}. The sum S is carried to $l=1350$.

System	T (K)	N_i (cm^{-3})	R_m (Å)	S (10^3)	z
KCl:Sr^{2+}	900	10^{17}	118.17	35.613	1.198
CaF_2:RE^{3+}	900	10^{17}	110.35	24.684	1.100
	1100	10^{17}	103.68	15.179	1.062
	1300	10^{17}	97.50	9.888	1.040
	1500	10^{16}	128.02	10.577	1.004
	1500	10^{17}	91.85	7.240	1.029
	1700	10^{15}	135.19	9.141	1.000
	1700	10^{16}	117.18	8.084	1.003
	1700	10^{17}	86.69	5.569	1.023

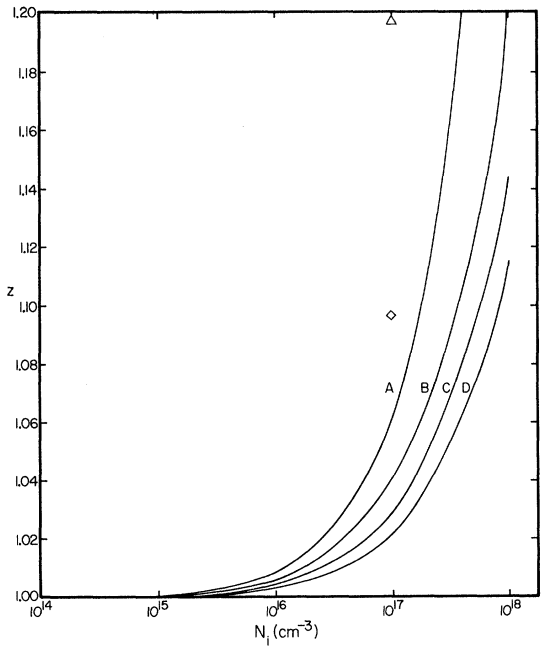

FIG. 1. Variation of z with N_i at 1100 K (A), 1300 K (B), 1500 K (C), and 1700 K (D) for CaF_2:RE^{3+}. The symbols ◇ and △ represent calculations for the CaF_2:RE^{3+} and KCl:Sr^{2+} systems at 900 K, respectively.

IV. LOW-TEMPERATURE PAIR DISTRIBUTION CURVES

The results of the high-temperature treatment given in Secs. II and III differ in a fundamental manner from those of the low-temperature treatment. From the high-temperature treatment, the concept of pair correlation functions evolves which leads to the total number ${}^{\pm}n_l^*$ of pair interactions at a distance R_l between the interacting ions [Eq. (25) and Figs. 2 and 3]. The effect of the presence of other ions about a given cation in the high-temperature treatment thus, in essence, averages out isotropically, so that the cubic environment of the host lattice becomes the dominant perturbation for the crystal field symmetry. In the low-temperature limit, however, the picture is one of cation-defect pairs, and the cubicity about the cation is lowered to some symmetry prescribed by the position of the defect relative to the cation. In this section we shall first extend the low-temperature distribution calculation to several crystalline ionic solutions in order to observe certain trends. The fundamental differences between the high- and low-temperature treatments will be discussed in the closing paragraphs in Sec. V.

At low temperature and high dilution, screening due to other impurity-defect pairs may be ne-

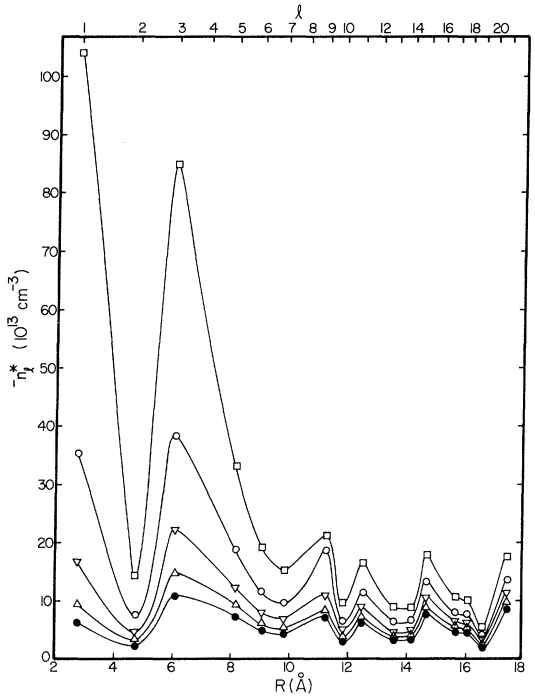

FIG. 2. Number $^{-}n_l^*$ of attractive pair interactions for $l \leq 21$ at 900 K (□), 1100 K (○), 1300 K (▽), 1500 K (◇), and 1700 K (●). The curves connecting the points are shown as a visual guide and are not to be taken as part of the calculations.

glected,[1] and the interaction energy u_l may be regarded as purely Coulombic for all but the first and second nearest-neighbor (nn) pairs.[8] The departure from a purely Coulombic potential at small values of l is due to the repulsive interaction from electron overlap and to the polarization of the lattice about the impurity-defect pair. Values for u_1 and u_2, the first and second nn interaction energies, have been calculated or measured for the following systems: NaCl:Sr^{2+} ($u_1 = -0.45$ eV, $u_2 = -0.41$ eV),[8] NaCl:Mn^{2+} ($u_1 = -0.3$ eV, $u_2 = -0.35$ eV),[9] and LiCl:Mn^{2+} ($u_1 = -0.3$ eV, $u_2 = -0.26$ eV).[9] Using these values and Eq. (4), we have calculated site symmetry distributions with q_p summed to $l' = 200$ in the manner previously described.[1] The results are shown in Figs. 4–6.

From Figs. 4–6 and the distribution curves previously determined for the KCl:Sr^{2+} system,[1] we observe that as the size of the impurity ion decreases, or conversely as the lattice spacing of the host increases, the second nn compensation becomes increasingly more probable. Although the unavailability of u_1 and u_2 for (alkaline-earth halide):RE^{3+} systems other than CaF_2[2] deprives us of detailed calculations of site symmetry distributions, electron paramagnetic resonance (EPR) investigations have revealed a similar trend in these systems.[10,11] For example, first nn compensation was not observed for the BaF_2:Yb^{3+}[10] and BaF_2:Gd^{3+}[11] systems, while the probability for the first nn compensation in CaF_2:RE^{3+} systems is found to be predominant.[2] An explanation of this trend can be given by considering one of the terms contributing to the binding energies of the first and second nn pairs. This term, introduced by Brauer,[12] considers the effect of the size of the impurity ion on the binding energy of the pair. It accounts for the fact that the perturbing impurity ion is not only a source of electrostatic polarization, but, as its ionic radius may be quite different from that of the cation it has replaced, it may also be a source of displacement polarization. Each ion in the surrounding lattice undergoes a purely elastic displacement and consequently produces a displacement dipole which has the net effect of altering the binding energies of the impurity-defect pairs. When the impurity ion decreases in size, the nn shell of host anions, in particular, will be displaced inward. These displacement dipoles will have the effect of increasing the shielding between the impurity ion and its first nn defect compensations, thus reducing u_1. The quantity u_2, on the other hand, will increase as the second nn defect moves closer to the impurity ion due to the inward displacement of the nn host anions, thus accounting for the observed changes in the relative abundance of the first two nn pairs. The conditions under which the results discussed in the

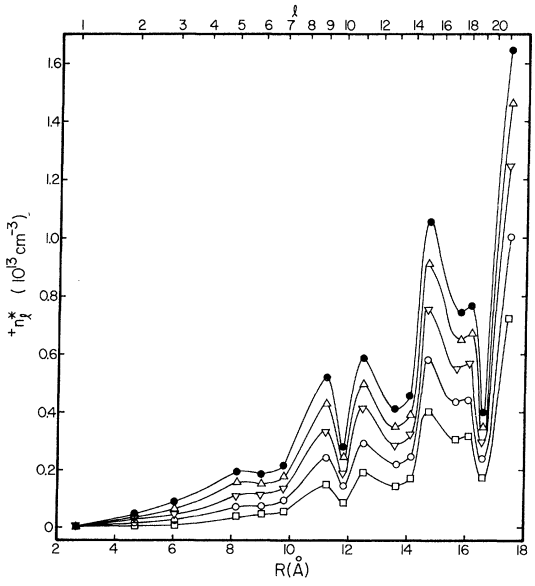

FIG. 3. The number $^{+}n_l^*$ of repulsive pair interactions for $l \leq 21$ at 900K (□), 1100 K (○), 1300 K (▽), 1500 K (◇), and 1700 K (●).

present section are valid will be elaborated in Sec. V.

V. DISCUSSION

The high-temperature treatment given in this work is valid under the condition Eq. (28), which will be satisfied at high temperature and high dilution. In the Debye-Hückel theory, the basic assumption is that ${}^{\pm}G(R) = e^{\mp u(R)/kT}$ which is, in essence, the same statement as Eq. (24). Our high-temperature treatment thus lends itself to comparison with the Debye theory, except that the discreteness of the crystalline lattice provides us with a unique handle on the evaluation of the pair correlation functions ${}^{\pm}G(R_l)$ and ${}^{\pm}n_l^*$.

The low-temperature treatment[1] reviewed in Sec. I and further elaborated in Sec. IV, on the other hand, is completely different in nature. If equilibrium conditions are attained at finite ionic concentrations, ions of opposite charges will pair as temperature decreases through attractive Coulombic interactions. At sufficiently low temperatures these ion pairs will cluster through higher polar interactions such that precipitation eventually results. This is the case, for example, in an aqueous solution of KCl. In crystalline ionic solutions of the type described in the present paper, however, true equilibrium is not readily attainable at low temperatures due to the low mobilities of the aliovalent cations. These cations are, in fact, "frozen" in a metastable equilibrium characteristic

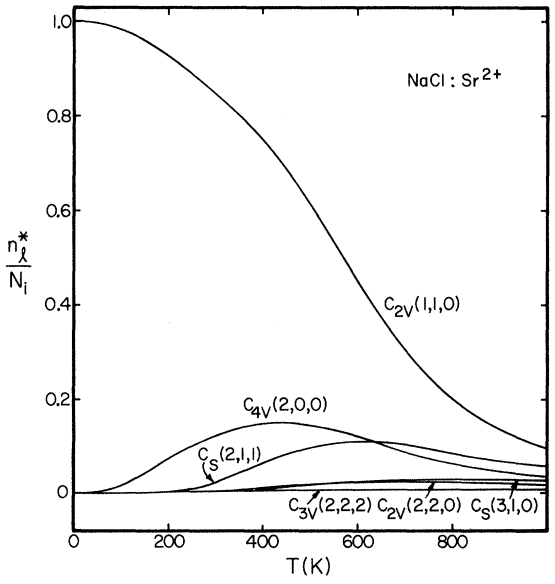

FIG. 4. Probabilities n_l^*/N_i of finding $C_{2v}(1, 1, 0)$, $C_{4v}(2, 0, 0)$, $C_s(2, 1, 1)$, $C_{2v}(2, 2, 0)$, $C_s(3, 1, 0)$, and $3_{3v}(2, 2, 2)$ sites in NaCl : Sr^{2+} (Sr^{2+} ionic radius = 1.13 Å; Na^+ ionic radius = 0.95 Å). The symmetry notations have been explained in Ref. 1.

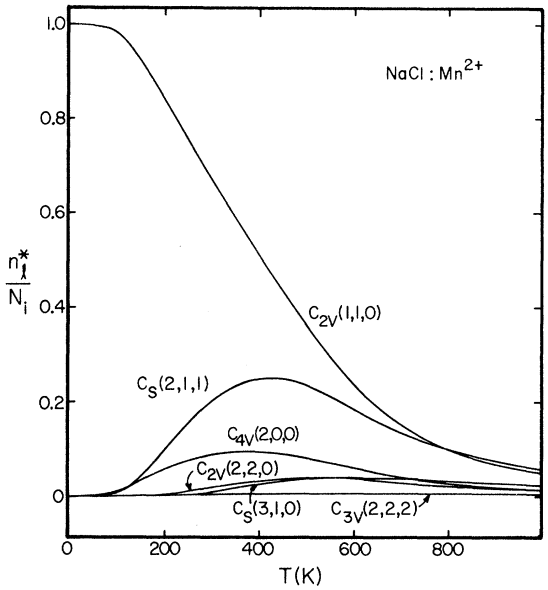

FIG. 5. Probabilities n_l^*/N_i of finding $C_{2v}(1, 1, 0)$, $C_{4v}(2, 0, 0)$, $C_s(2, 1, 1)$, $C_{2v}(2, 2, 0)$, $C_s(3, 1, 0)$, and $C_{3v}(2, 2, 2)$ sites in NaCl : Mn^{2+} (Mn^{2+} ionic radius = 0.8 Å; Na^+ ionic radius = 0.95 Å).

of some higher temperature, in which they are well dispersed throughout the entire lattice. The associated defects (i.e., the anions), on the other hand, possess much greater mobilities so that they can equilibrate through attractive Coulombic forces in pair formation with the cations. For example, the K^+ vacancy in KCl has a migrational activation energy of 0.63 eV.[9] Assuming the value 10^{14} given[13] for the preexponential frequency factor for the jump of a K^+ vacancy from one lattice position to an adjacent one, the time required for thermal equilibration of the vacancy about a divalent cation will be on the order of 10^{-3} sec at 300 K.[14] We thus visualize the formation of cation-defect pairs which cannot aggregate through higher polar attractions at low temperatures. In some proper temperature range, therefore, we have N_i pairs whose mutual interactions are negligibly small (at sufficiently high dilution), and Eq. (3) results. The conceptual model depicted in Eq. (3) requires that the ensemble of ions is divided into N_i cells, each of which containing one ion-defect pair. The "molecular" pair partition function q_p must be summed over all $(N/N_i - 1)$ lattice points per cell. The model will be valid if the occupation probability is significant only for the first few nn positions, i.e.,

$$q_p = \sum_{l=1}^{l=l'} g_l e^{-u_l/kT} \gg \frac{N}{N_i} . \tag{32}$$

For example, $q_p \sim 10^8$ and 10^5 at 300 and 500 K, respectively, for KCl:M^{2+}. For $N_i = 10^{17}$ cm^{-3}, $N/$

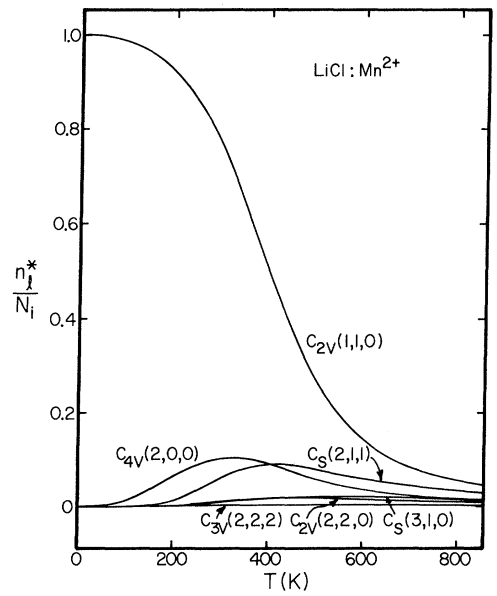

FIG. 6. Probabilities n_i^*/N_i of finding $C_{2v}(1, 1, 0)$, $C_{4v}(2, 0, 0)$, $C_s(2, 1, 1)$, $C_{2v}(2, 2, 0)$, $C_s(3, 1, 0)$, and $C_{3v}(2, 2, 2)$ sites in LiCl : Mn^{2+} (Mn^{2+} ionic radius = 0.8 Å; Li ionic radius = 0.60 Å).

$N_i \sim 10^3$, and Eq. (3) is thus valid for $T \lesssim 500$ K if pair formation equilibrium is attained. (At $T \ll 300$ K even the K^+ vacancy mobility will be too low for thermal equilibration.) At higher dilution, Eq. (3) will be valid at lower temperatures.

Finally, we return to the high-temperature results in an assessment of their applicability to real systems. The calculations have been made at sufficiently high dilution (10^{17}–10^{18} cm^{-3}) and temperatures ($T \geq 900$ K) in order to ascertain the condition stated in Eq. (28). The concentrations of intrinsic defects were ignored in all our calculations for the sake of simplicity. In reality, however, these concentrations are by no means negligible at $T \geq 900$ K. In KCl and CaF_2, for example, the intrinsic defect concentrations are on the order of 10^{16} cm^{-3} [13] and 10^{17} cm^{-3} [15,16] at 900 K, respectively. It is therefore necessary to extend our treatment to include the interactions due to the presence of intrinsic defects in the evaluation of Z, which presents no serious difficulties. At $T > 900$ K, however, the intrinsic defect concentrations in CaF_2 exceed the range in which Eq. (28) is valid, being as high as $\sim 10^{20}$ at $T = 1300$ K. An adequate treatment of such a situation would require an inclusion of the "other terms" in Eq. (14). The results reported in Secs. II and III nevertheless represent a quantitative, albeit idealized, *approach* to the fairly complex problem of interacting dissociated ions in a periodic crystalline lattice. Equally important is the fact that through the contrast between these results and those obtained through the low-temperature partition function Z of Eq. (3), several novel features of the pair distribution theory have been elucidated. The spectroscopic observation of the predominance of "cubic" sites in CaF_2:RE^{3+} systems when they are quenched[2] from elevated temperatures is, in fact, experimental evidence of the results shown in Figs. 2 and 3. At $T = 900$ K and $N_i = 10^{17}$ cm^{-3}, only $\sim 2\times10^{15}$-cm^{-3} ion-defect pairs are within $l \leq 21$ (Fig. 2). Since the compensation crystal field potential varies as $R_i^{-(k+1)}$ where $k > 0$ is the rank of the spherical harmonic in the corresponding crystal field potential expansion, the crystal field effect of the more distant compensation sites would be negligibly small as the cubic environment of the RE^{3+} ion becomes the dominant factor in the spectroscopic observations. The predominance of cubic sites in CaF_2 (which is not observed in the KCl:M^{2+} systems[1,3-6]) arises from the high migrational activation energy 1.51 eV[17] of the compensation F^- interstitials. At 600 K, the time required for thermal equilibration of the site distribution characteristic of the low-temperature range is ~ 1 sec. At room temperature (~ 300 K), however, the time required for thermal equilibration is on the order of 10^7 years.[2] Rapid quenching to room temperature, therefore, would cause freezing of the high-temperature equilibrium depicted in Figs. 2 and 3 in a metastable equilibrium. In view of the present discussion, it appears certain that quenching from elevated temperatures of alkali halide: M^{2+} systems to $T \ll 300$ K should also give rise to a predominance in cubic sites, which characterize the high-temperature equilibria.

---

*This research was supported under the institutional ARPA Grant No. SD102.

[1]F. K. Fong, Phys. Rev. 187, 1099 (1969).
[2]R. H. Heist and F. K. Fong, Phys. Rev. B 1, 2970 (1970).
[3]F. K. Fong, Phys. Rev. B 1, 4157 (1970).
[4]F. K. Fong and J. C. Bellows, Phys. Rev. B 1, 4240 (1970).
[5]F. K. Fong, R. H. Heist, C. R. Chilver, J. C. Bellows, and R. L. Ford, J. Luminescence 1, 889 (1969).
[6]F. K. Fong and E. Y. Wong, Phys. Rev. 162, 348 (1967).
[7]N. Davidson, *Statistical Mechanics* (McGraw-Hill, New York, 1962), Chap. 15.
[8]J. R. Reitz and J. L. Gammel, J. Chem. Phys. 19, 894 (1951); F. Bassani and F. G. Fumi, Nuovo Cimento 11, 274 (1954); M. P. Tosi and G. Airoldi, *ibid.* 8, 584 (1958).
[9]G. D. Watkins, Phys. Rev. 113, 79 (1959); 113, 91 (1959).
[10]U. Ranon and A. Yariv, Phys. Letters 9, 17 (1964).
[11]J. Sierro, Phys. Letters 4, 178 (1963).

[12]P. Brauer, Z. Naturforsch. 6A, 255 (1951).
[13]R. W. Dreyfus and A. S. Norwick, Phys. Rev. 33, 437 (1962).
[14]There is some question in this estimate due to the uncertainty in the migrational barrier for the K^+ vacancy migration. The value 0.63 eV given by Watkins (Ref. 9) corresponds to the migration of a K^+ vacancy in the close proximity of the divalent cation. In an ionic conductivity experiment H. W. Etzel and R. J. Maurer [J. Chem. Phys. 18, 1003 (1950)] reported the value 0.85 eV for the migrational barrier of Na^+ vacancy in NaCl. The higher value reported by these authors probably corresponds to free-vacancy migration. Employing the value 0.85 eV in our estimate, the time required for thermal equilibrium of the vacancy about a divalent cation will be on the order of 2 sec at 300 K. The main argument in the text thus remains unaffected.
[15]R. W. Ure, Jr., J. Chem. Phys. 26, 1363 (1957).
[16]F. K. Fong, *Progress in Solid State Chemistry*, edited by H. Reiss (Pergamon, New York, 1966), Vol. III, Chap. 4.
[17]F. K. Fong and M. A. Hiller, J. Phys. Chem. 71, 2854 (1967).

PHYSICAL REVIEW B VOLUME 2, NUMBER 10 15 NOVEMBER 1970

Polarons Bound in a Coulomb Potential. II. 2*P*-State Zeeman Effect*

David M. Larsen
Lincoln Laboratory, Massachusetts Institute of Technology, Lexington, Massachusetts 02173
(Received 1 April 1970)

Approximate polaron effective-mass trial functions are constructed to describe 2*P* hydrogenic polaron levels in weak magnetic fields. Breakdown of the effective-mass description due to level crossing of the 2*P* effective-mass states with 1*S* one-phonon states [denoted (1*S*, 1)] necessitates admixture of (1*S*, 1) states to the initial effective-mass state in order to achieve lowest cariational energy. The effect of mixing in the (1*S*, 1) states is to produce, effectively, a double-values 2*P* energy and to reduce considerably the linear Zeeman splitting near the point of level crossing. Level crossings with (1*S*, *n*) states for $n>1$ are expected, on the basis of a heuristic argument, to produce similar discontinuities near the respective crossing energies. Perturbation theory is used to find expressions in the weak-coupling limit for the Zeeman splitting in the limit of weak binding, and, for stronger binding, near the (1*S*, 1) level crossing.

I. INTRODUCTION

A slowly moving electron in the conduction band of a polar crystal finds itself surrounded by lattice polarization charge induced by the electron's own Coulomb field. Treating the lattice as a polarizable continuum one can show[1] that in the simple case of a parabolic conduction band the electron-lattice (or more precisely, electron–LO-phonon) coupling strength is characterized by a dimensionless constant α, given by

$$\alpha=\frac{1}{2}\left(\frac{1}{\epsilon_\infty}-\frac{1}{\epsilon_0}\right)\frac{e^2}{(r_0\hbar\omega)}\,, \tag{1}$$

where $r_0=(\hbar/2m\omega)^{1/2}$. The length r_0 turns out to be essentially the radius of the polarization charge distribution surrounding the slowly moving electron (unless α is very large). This complex of electron plus polarization cloud is the so-called polaron. We have used m for the electron band mass, $\hbar\omega$ for the energy of a long-wavelength LO phonon, and ϵ_∞ and ϵ_0 for the high-frequency and static dielectric constants, respectively, of the lattice.

If α is not too large, the polaron energy, which in the absence of interaction is simply $p^2/2m$, becomes with interaction

$$E(p)=-\alpha\hbar\omega+\frac{p^2}{2m(1+\alpha/6)}-\frac{3\alpha}{160}\frac{p^4}{m^2\hbar\omega}+O\left(\frac{\alpha p^6}{m^3(\hbar\omega)^2}\right). \tag{2}$$

Thus, carriers in a nominally parabolic conduction band will behave as if the band were, in fact, nonparabolic, due to the terms in (2) proportional to p^4, p^6, etc.

Polaron-induced nonparabolicity has been clearly demonstrated by cyclotron-resonance experiments in InSb[2,3] and CdTe.[4] In these experiments, the magnetic analog of $E(p)$ is probed by measuring the $n=0$ to $n=1$ Landau-level energy separation as a function of magnetic field.

Perhaps the most striking aspect of polaron nonparabolicity is the pinning phenomenon[5] observed at fields large enough to bring the unperturbed ($\alpha=0$) cyclotron frequency close to ω. At such fields, the cyclotron resonance appears to split into two branches, one always lying above $\hbar\omega$ in energy, the other always below. The lower-branch energy approaches $\hbar\omega$ with increasing field, while at the same time the upper-branch frequency becomes close to the unperturbed cyclotron frequency.